Base Station Orientation Calibration in 3-D Indoor UWB Positioning

Brandon Merkl[1], Aly Fathy[2], and Mohamed Mahfouz[1]

[1]Department of Mechanical, Aerospace, and Biomedical Engineering, [2]Department of Electrical Engineering and Computer Science, University of Tennessee, Knoxville, Tennessee, 37996, USA

***Abstract* — A method is proposed to correct three-dimensional (3D) positioning error due to base station antenna orientation that takes into account non-boresight electrical length differences due to antenna phase center errors. An automated algorithm is used to calibrate an ultra-wideband (UWB) system using only a starting estimate of the base station position and acquired positions central to the base stations. The true positions of the acquired 3D calibration points are unknown to the calibration algorithm. Upon completion of the algorithm, the base station orientation is estimated, along with estimates of electrical length offsets due to potential cable length differences. This method is designed to minimize small errors due to base station position and orientation uncertainty. The algorithm is shown to be robust given the availability of accurate 1D ranging can be provided by the system.**

***Index Terms* — Phase center error, base station orientation, 3D localization**

I. Introduction

In designing and constructing a high accuracy (~1mm) UWB positioning system [1,2], several types of errors and biases that are safely ignored on the decimeter scale, become significant to overall system performance. One such effect is that of phase center errors originating from transmitter-receiver mal-alignment. It will be shown these errors can be successfully removed using the Time-Difference-of-Arrival (TDOA) algorithm with knowledge of the receiving antenna orientations; however, ignoring this type of error proves impossible for the TDOA algorithm to remove. Even in a trial case involving 100 base stations, phase center errors are correlated and create considerable system error. Thus, the accuracy of the TDOA algorithm is highly dependent on the accuracy of the differences in the time of arrival (TOA) of our ultra-wideband pulses.

Using an iterative approach, an algorithm has been developed and tested under simulated line-of-sight (LOS) conditions where ranging error was modeled as a zero mean Gaussian random variable with a variance equal to the amount of ranging error present in our UWB system.

II. Previous Work

Much prior work has been done in the field of UWB positioning. Currently, commercial UWB positioning systems of Sapphire DART (Multispectral Solutions, Inc.) and Ubisense have indoor positioning accuracy of 10 cm and 15 cm, respectively [3,4]. Interesting results presented by Zetik et al. and Meier et al. indicate that ranging has the potential to achieve mm or even sub-mm accuracy levels [5,6]. Recent work in UWB positioning algorithms has focused on increasing the accuracy of TOA measurements in Non-Line-of-Sight (NLOS) conditions [7], increasing TOA resolution [8], and increasing TOA accuracy in the presence of interference [9].

III. Materials and Methods

The purpose of the experiments described previously is to expose and eliminate the error due to antenna phase center and simultaneously positioning error due in the antenna bore sight direction uncertainty. First, a short discussion of the phase center error is included for relevance to this calibration procedure.

A. Antenna Phase Center Error

The single element Vivaldi antenna is used on the receiver side of our system. The design of the antenna is shown below in Fig 1.

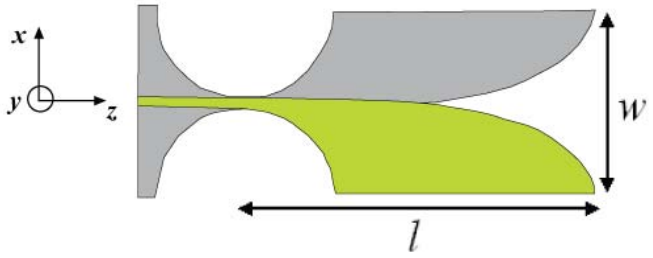

Fig. 1. Designed Vivaldi antenna, with the +z axis being the boresight direction

The z-axis points in the direction of the “end fire” radiation pattern typical of antipodal antennas. This particular design of antenna is particularly sensitive to phase center variation in both the E-plane (parallel with the plane of the antenna, xz-plane in Fig. 1) and H-plane of the antenna radiation pattern as shown in Figure 2 [1].

978-1-4244-1827-5/08/$25.00 ©2008 IEEE

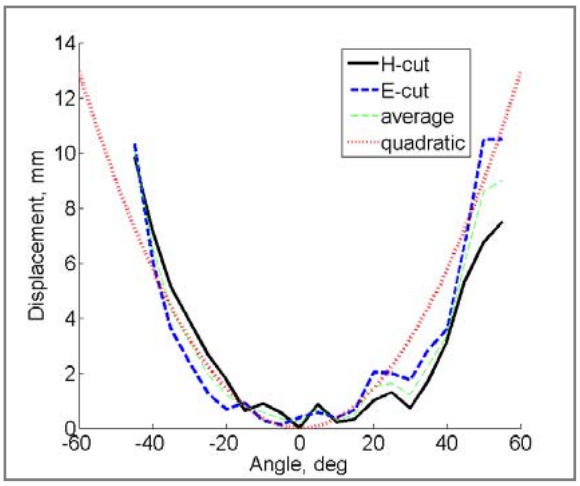

Fig. 2. Measured Vivaldi phase center error versus angle for E-cut, H-cut, average of E and H cuts, and centered quadratic fit

The average error between the E-cut and H-cut are used to approximate the error as a function of any angle of incidence relative to the boresight direction. A quadratic approximation was chosen and is of the form

$$\Phi = E(\theta) = 0.00000364(\theta)^2 \quad (1)$$

where θ is calculated as the full angle in degrees between the angle of incidence and the boresight direction and Φ is positioning error in meters.

B. Orientation Error Simulation

An experiment was undertaken to discover the effects of the phase center error on the TDOA algorithm when combined with a large amount of base stations. In this case, it was hypothesized that the redundancy in the large number of base stations would tend to cancel out the phase center errors.

In this simulation a virtual scene is created with $N=100$ base stations randomly distributed on a sphere of radius R=3 m. In this experiment base stations are assumed to all be oriented directly toward the center of the sphere, which is the origin of the coordinate system (0,0,0). The tag travels in a helical path between x-axis values of $\pm R/2$ according to

$$P_i^T = \left(x_i, r_i \sin(w_H x_i), r_i \cos(w_H x_i)\right) \quad (2)$$

$$r_i = \min\left(\frac{x_i}{2}, r_{MAX}\right) \quad (3)$$

where x_i are M=81 uniformly sampled points between $x=\pm R/2$. A particular instance of this recreated scene is shown in Figure 3. Given the tag positions and the base stations positions, the true 1D range is calculated for each tag position relative to each base station. Also, the true angle of incidence is known and calculated for each tag position-base station pair. Synthetic range values are thus calculated as

$$d_{ij}^{TBS} = \left\| P_i^T - P_j^{BS} \right\| + \Phi_{ij} + b_j + n_{ij} \quad (4)$$

where $1 \le i \le M$, $1 \le j \le N$ and P_j^{BS} represents the position of the j^{th} base station, Φ_{ij} is the phase center error between the i^{th} tag position and j^{th} base station. A Gauss-distributed random bias term b_j (μ=0, σ=2.5 mm) is added to the range to account for potential electrical length differences, and the slight uncertainty in measuring the base station position phase center along the boresight direction. The nominal value for the standard deviation was chosen to be an order of magnitude higher than the uncertainty of 3D localization. Finally, a random noise figure of n_{ij} (μ=0, σ=1.24 mm) is added to each range to account for uncertainty in 1D range measurements. This nominal value was chosen based on the actual 1D measurement RMS error of our system [2].

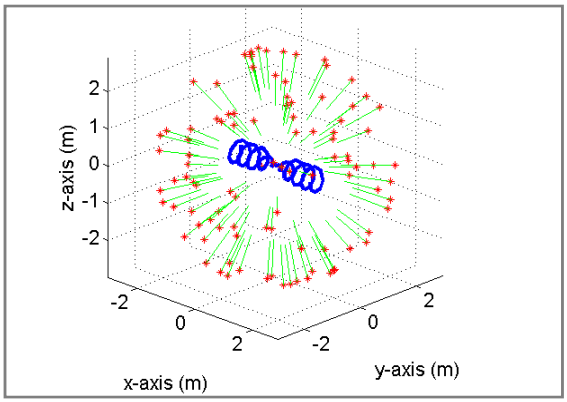

Fig. 3. Instance of the 100 base station experiment

In this simulation, the standard TDOA algorithm is applied to the synthetic ranges generated in (4), and the error of the calculated position vs. the true position as a function of the x_i position of P_i^T is shown in Fig. 4.

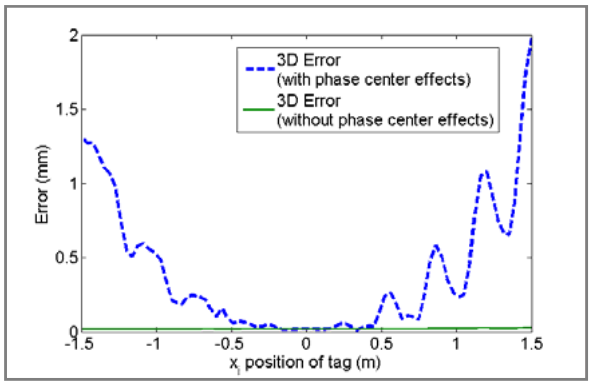

Fig. 4. 3D Positioning Error vs. Tag x_i Position for 100 base station experiment illustrating the difference between Φ included (dashed) and not included (solid) in equation (4)

According to Figure 4, redundancy in the number of base stations is not sufficient to remove phase center error. This can also be understood by considering that the geometry at both extremes of the tag path represent cases where many of the base stations will simultaneously have significant phase center error that creates a positive length bias that the TDOA algorithm cannot remove.

C. Calibration Algorithm

Considering the same geometry as described in the previous simulation, it is desirable to calibrate the system to determine accurately the orientation of the base stations only through measured data. Assuming that the base stations are again oriented roughly toward the center of the work area and that the base stations positions are known, the proposed algorithm will estimate both the orientation and boresight bias (b_j) according to the error model given in equation (4). Also, to perform this calibration there must be N>4 base stations, as one base station must be left out. This leaves a minimum of 4 base stations to provide unambiguous hyperbolic 3D positioning.

Algorithm 1: Phase Center TDOA Calibration

---

1. Using the raw 1D ranging values, use the TDOA algorithm on *N-1* base stations (leaving one base station out of the calculations). Iterate so that each base station is left out in turn. This is performed at all tag positions. The result is *MN* position estimates $\hat{P}_{ij}^{T}$, for the i^{th} position corresponding to the j^{th} base station that was removed. All of the base stations are given an initial orientation estimate $\hat{O}_j^{BS}$ which is a random unit vector, representing the boresight direction.
2. Each position estimate $\hat{P}_{ij}^{T}$ is used to calculate the angle θ_{ij} between the tag position-base station and the current orientation estimate $\hat{O}_j^{BS}$.

3a. We estimate the true 1D ranging values $\hat{R}_{ij}$ based on the calculated θ_{ij}

$$\hat{R}_{ij} = R_{ij} - E(\theta_{ij}) - \hat{b}_j \tag{5}$$

where R_{ij} is the measured range and $\hat{b}_j$ is the current estimate of the boresight bias (initially set to zero).

3b. Alternatively, we also estimate the error due to the phase center $\hat{\Phi}_{ij}^{TBS}$ without consideration of the current orientation

$$\hat{\Phi}_{ij}^{TBS} = R_{ij} - \hat{P}_{ij}^{T} - \hat{b}_j \tag{6}$$

and subsequently,

$$\hat{\theta}_{ij} = \begin{cases} E^{-1}\left(\hat{\Phi}_{ij}^{TBS}\right) & \hat{\Phi}_{ij}^{TBS} > 0 \\ 0 & \hat{\Phi}_{ij}^{TBS} \le 0 \end{cases} \tag{7}$$

noting that this step can be performed independently of step 3a.

4. The estimated ranging values $\hat{R}_{ij}$ are then used in the standard TDOA algorithm to re-estimate position values $\tilde{P}_i^T$ using all *N* base stations in the calculation.
5. The collection of position estimates $\tilde{P}_i^T$ is then used to update the boresight bias estimate

$$\hat{b}_j = \hat{b}_j^{old} + \frac{1}{M}\sum_{i=1}^{M}\left(\left\|\tilde{P}_i^T - P_j^{BS}\right\| - \hat{R}_{ij}\right) \tag{8}$$

which can be considered as an update to the existing bias estimate using the mean ranging error across all measured positions.

6. Next the orientation estimate $\hat{O}_j^{BS}$ is updated according to:

$$K_j = \min\arg_i\left(\sum_{k=1}^{N}\hat{\theta}_{ik}\right) k \neq j \tag{9}$$

$$\hat{O}_j^{BS} = \left(\tilde{P}_{K_j}^T - P_j^{BS}\right) / \left\|\tilde{P}_{K_j}^T - P_j^{BS}\right\| \tag{10}$$

thus, the final step in this iterative algorithm is to assign the base station orientations according to the points along the point track where the *N-1* base station positions yield the lowest amount of angular error. Under the assumption that the base stations are oriented roughly towards the center of the work area, this condition yields algorithm convergence.

7. The algorithm converges when the relative RMS error between position estimates falls below a threshold.

D. Calibration Simulations

Several simulations under realistic system configurations were used to verify the accuracy and convergence characteristics of Algorithm 1, for calibrating the base station orientations and electrical length differences. These trials were enacted under a varied number of base stations randomly distributed on a sphere. Several fixed parameters set in this study were: the minimum resolvable distance (0.1 mm), the noise in 1D measurement (1.24 mm), and the number of trials for each

configuration (20 trials). The 1D ranging noise was taken from observed 1D ranging noise in [2].

IV. Results

The algorithm was monitored and averaged across the 20 trials to give a relative indicator of success. Two such trials are shown in Figure 5. In the first case which represented only 6 base stations, there was not a sufficient level of redundancy for the algorithm to converge to sub-mm range calibrated error. This is due in part to occasional dilutions of geometric precision which causes instability in the algorithm to ascertain correct ranging values. While on average the *N=6* case did not converge to sub-mm levels of accuracy, most of the runs did converge with the mean being negatively influence by a few cases of non-convergence.

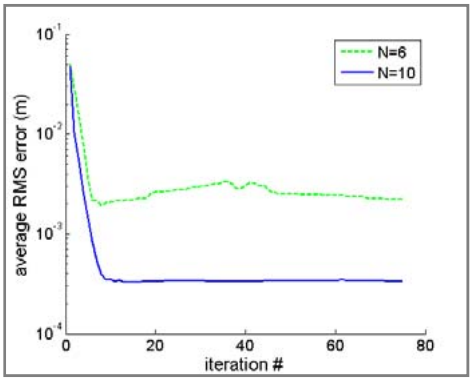

Fig. 5. Comparison of N=6 base stations and N=10 base stations on the calibration algorithm convergence. Note algorithm instability for N=6 case. Sub-mm calibrated accuracy is possible with N=10 base stations

From Figure 5 it is clear that the *N=10* base station case represented enough system redundancy to drastically reduce noisy 1D ranging errors (1.24 mm) with the limit being the (0.1 mm) minimum resolvable distance being preserved.

V. Discussion

The system calibration procedure described in this paper is necessary to push the limits of UWB positioning beyond the current levels of commercial accuracy. The algorithm was tested in simulated LOS conditions where measurement error is well-known to be minimal. It would remain to be further work to test the algorithm in situations of non-line-of-sight (NLOS) conditions, as well as situations where the base station orientations cannot be assumed to be oriented toward the center of the work area. While much work in UWB positioning has been performed in driving raw 1D TOA accuracy, with many associated algorithms being developed in the literature, the authors' wish is to motivate a careful look at antenna phase center effects on overall system accuracy. The algorithm presented here describes a calibration procedure that can be translated into TDOA based positioning systems where AOA effects result in system degradation of accuracy. In such systems, the orientation of the base station relative to the mobile tag can be inferred as well as biases resulting in fixed electrical length differences. Such differences could arise if different lengths of cable are used to connect the base stations, or if the base stations retransmit pulse arrival times. The prime feature of the proposed algorithm is that arbitrarily captured points can be used to calibrate the system, which indicates that this algorithm may be able to be implemented as a continuous online process or purely performed offline. The drawback to this technique would be the relatively large degree of redundancy that must be present in the system.

References

[1] M. Mahfouz, C. Zhang, B. Merkl, M. Kuhn, A. Fathy, "Investigation of high accuracy indoor 3-D positioning using UWB technology," *Accepted*, IEEE Trans Microwave Theory & Tech, to be published 2008.

[2] C. Zhang, M. Kuhn, B. Merkl, M. Mahfouz, and A. E. Fathy, "Development of an UWB indoor 3-D positioning radar with millimeter accuracy," in IEEE MTT-S International Microwave Symposium, 2006, pp. 106-109.

[3] Sapphire DART (RTLS) Product Data Sheet, Multispectral Solutions Inc., Germantown, MD, 2007, http://www.multispectral.com/pdf/Sapphire_DART.pdf

[4] Hardware Datasheet, Ubisense, Cambridge, UK, 2006, http://www.ubisense.net/SITE/UPLOAD/Document/TechDocs/Ubisense_hardware_datasheet_May_2006.pdf

[5] R. Zetik, J. Sachs, R. Thomä, "UWB localization - active and passive approach," in *Proceedings of the 21st IEEE IMTC*, vol. 2, 2004, pp. 1005-1009.

[6] C. Meier, A. Terzis, S. Lindenmeier, " A robust 3D high precision radio location system," in *IEEE MTT-S International Microwave Symposium*, 2007, pp. 397 – 400.

[7] J. Schroeder, S. Galler, K. Kyamakya, and T. Kaiser, "Three-dimensional indoor localization in non line of sight uwb channels," in *ICUWB* 2007.

[8] Zhou, Yuan; Guan, Yong Liang; Law, Choi Look; Xu, Chi, "High-Resolution UWB Ranging based on Phase-Only Correlator," *ICUWB* 2007.

[9] Dardari, Davide; Giorgetti, Andrea; Win, Moe Z., "Time-of-Arrival Estimation of UWB Signals in the Presence of Narrowband and Wideband Interference," *ICUWB* 2007.